

RESEARCH PAPER



Sesquiterpenoids and 2-(2-phenylethyl)chromones respectively acting as α -glucosidase and tyrosinase inhibitors from agarwood of an *Aquilaria* plant

Li Yang^{a,b}, Yi-Ling Yang^{a,b}, Wen-Hua Dong^{a,b,c}, Wei Li^{a,b,c}, Pei Wang^{a,b,c}, Xue Cao^{a,b}, Jing-Zhe Yuan^{a,b,c}, Hui-Qin Chen^{a,b,c}, Wen-Li Mei^{a,b,c} and Hao-Fu Dai^{a,b,c}

^aKey Laboratory of Biology and Genetic Resources of Tropical Crops, Ministry of Agriculture, Institute of Tropical Bioscience and Biotechnology, Chinese Academy of Tropical Agricultural Sciences, Haikou, People's Republic of China; ^bHainan Key Laboratory for Research and Development of Natural Products from Li Folk Medicine, Haikou, People's Republic of China; ^cHainan Engineering Research Center of Agarwood, Haikou, People's Republic of China

ABSTRACT

The ethyl ether extract of agarwood from an *Aquilaria* plant afforded six new sesquiterpenoids, Agarozizanol A–F (**1–6**), together with four known sesquiterpenoids and six known 2-(2-phenylethyl)-chromones. Their structures were elucidated via detailed spectroscopic analysis, X-ray diffraction, and comparisons with the published data. All the isolates were evaluated for the α -glucosidase and tyrosinase inhibitory activities *in vitro*. Compounds **5**, **7**, **8**, and **10** showed significant inhibition of α -glucosidase with IC₅₀ values ranging between 112.3 ± 4.5 and 524.5 ± 2.7 μ M (acarbose, 743.4 ± 3.3 μ M). Compounds **13** and **14** exhibited tyrosinase inhibitory effect with IC₅₀ values of 89.0 ± 1.7 and 51.5 ± 0.6 μ M, respectively (kojic acid, 46.1 ± 1.3). In the kinetic studies, compounds **5** and **14** were found to be uncompetitive inhibitors for α -glucosidase and mixed type inhibitors for tyrosinase, respectively. Furthermore, molecular docking simulations revealed the binding sites and interactions of the most active compounds with α -glucosidase and tyrosinase.

ARTICLE HISTORY

Received 17 December 2018
Revised 18 January 2019
Accepted 27 January 2019

KEYWORDS

Agarwood; *aquilaria* plant; sesquiterpenoid; 2-(2-phenylethyl)chromone; α -glucosidase inhibition; tyrosinase inhibition

Introduction

Type 2 diabetes mellitus (T2DM), a chronic metabolic disorder disease, can cause life-threatening long-term complications including heart disease, strokes, blindness, kidney failure, and poor blood flow in the limbs¹. In 2015, an estimated 1.6 million deaths directly resulted from diabetes, which is among the top 10 causes of death worldwide². α -Glucosidase (EC 3.2.1.20) is an exo-acting enzyme, which implicates in the glycoprotein processing and carbohydrate metabolism. Additionally, α -glucosidase catalyzes the cleavage of α -1,4 glycosidic bonds from the nonreducing ends of oligosaccharides and provides high amount of intestine absorbable glucose, which results in the postprandial hyperglycaemia and complications associated with T2DM^{3,4}. Therefore, α -glucosidase inhibition is a very effective therapy to delay glucose absorption and lower blood glucose level after food intake, which can potentially postpone the progression of T2DM⁵.

As a precious traditional Chinese medicine, agarwood has been used for the treatment of joint pain, inflammatory related ailments, and diarrhoea, as well as a stimulant, sedative, and cardioprotective agent^{6–8}. It is also popular as an incense for cultural and religious ceremonies and its essential oil is further processed into perfume in cosmetics. Previous chemical studies revealed that sesquiterpenoids and 2-(2-phenylethyl)chromone derivatives are the two principal and aroma components in agarwood. To date, over 130 sesquiterpenoids and 120 2-(2-phenylethyl)chromone

derivatives have been isolated from agarwood⁹ and many of them exhibited various pharmacological properties including antibacterial¹⁰, anti-inflammatory¹¹, α -glucosidase inhibitory¹², acetylcholinesterase inhibitory¹³, cytotoxic¹², neuroprotective¹⁴, and antidepressant activities¹⁵. As part of our long-term project to chemically and biologically characterize chemical constituents from agarwood, the ethyl ether extract of agarwood from an *Aquilaria* plant was found to potently inhibit α -glucosidase. Then, a phytochemical investigation on the agarwood of an *Aquilaria* plant was performed and 10 α -glucosidase inhibitory sesquiterpenoids including 6 new sesquiterpenoids, Agarozizanol A–F (**1–6**), together with 4 known sesquiterpenoids (Figure 1) were isolated and identified. Additionally, 6 known 2-(2-phenylethyl)chromones were also obtained. 2-(2-Phenylethyl)chromones are structurally similar to the flavones except for presence of additional ethyl group and many flavones show intriguing tyrosinase inhibitory activity^{16–18}. Tyrosinase, a rate-limiting enzyme for the melanin biosynthesis, involves in pigmentation of skin¹⁹, browning in fresh vegetables and fruits²⁰, cuticle formation in insects^{21,22}, and neurodegeneration associated with Parkinson's disease²³. Hence, tyrosinase inhibitors have broad application in medicines, food preservatives, bio-insecticides, and cosmetic products. Inspired by this, All the 2-(2-phenylethyl)chromones were assayed for their tyrosinase inhibitory activity. Moreover, the inhibition mechanism were investigated. Herein, we report the isolation,

CONTACT Hao-Fu Dai  daihaofu@itbb.org.cn  Key Laboratory of Biology and Genetic Resources of Tropical Crops, Ministry of Agriculture, Institute of Tropical Bioscience and Biotechnology, Chinese Academy of Tropical Agricultural Sciences, Haikou 571101, People's Republic of China

 Supplemental data for this article can be accessed [here](#).

© 2019 The Author(s). Published by Informa UK Limited, trading as Taylor & Francis Group.

This is an Open Access article distributed under the terms of the Creative Commons Attribution License (<http://creativecommons.org/licenses/by/4.0/>), which permits unrestricted use, distribution, and reproduction in any medium, provided the original work is properly cited.

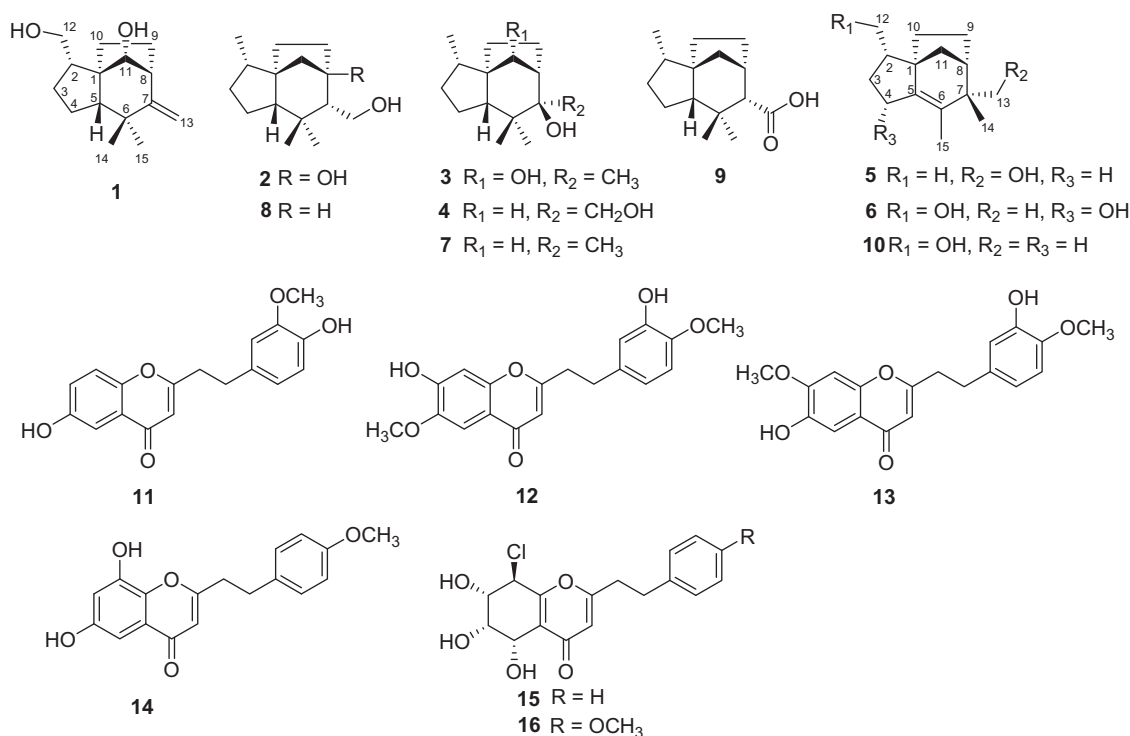


Figure 1. Structures of 1–16.

structure elucidation, α -glucosidase and tyrosinase inhibitory activities, as well as kinetic and molecular docking studies of these compounds.

Materials and methods

General experimental procedures

Optical rotations were measured on an Anton Paar MCP 5100 polarimeter. IR spectra were obtained using a Nicolet 380 FT-IR instrument (Thermo, USA) using KBr pellets. HRESIMS were determined by a Waters Autospec Premier (Waters, USA) mass spectrometer. The NMR spectra were recorded on Bruker Avance 500 NMR spectrometers (Bruker, Germany) with TMS as an internal standard. The high performance liquid chromatography (HPLC) was performed with an analytic reversed-phased column (YMC-packed C₁₈, 250 mm × 10 mm, 5 μ m) (YMC, Japan) using a G1311C 1260 Quat Pump VL and detected with a G1315D 1260 DAD VL detector (190–500 nm) (Agilent Technologies 1260 infinity, USA). For column chromatography, silica gel (60–80, 200–300 mesh, Qingdao Haiyang Chemical Co., Ltd, China), ODS gel (20–45 μ m, Fuji Silysia Chemical Co., Ltd, USA), and Sephadex LH-20 (Merck, Germany) were used. TLC analysis was performed on precoated silica gel GF254 plates (Qingdao Haiyang Chemical Co., Ltd, China), and spots were visualized by spraying with 5% H₂SO₄ in EtOH followed by heating. Thermo fisher scientific plate reader was used for enzyme inhibition assays.

Plant material

The agarwood was purchased from Bangkok, Thailand in August 2014 and its original plant was identified as a species of the genus *Aquilaria* by gene sequence analysis of the ITS region. A voucher specimen (201408SLLK) was retained at the Institute of Tropical Bioscience and Biotechnology, Chinese Academy of Tropical Agricultural Sciences.

Extraction and isolation

Air-dried agarwood (384.0 g) was ground and extracted with ethyl ether (1.5 L) for three times. The obtained extract was tested for the α -glucosidase inhibitory activity and showed inhibition rate of $44.13 \pm 1.92\%$ at concentration of 50 μ g/mL (acarbose, $62.06 \pm 4.77\%$). Then, the ethyl ether extract (20.4 g) was subjected to ODS column chromatography (CC) eluting with MeOH/H₂O (v/v, 2:3, 1:1, 3:2, 7:3, 4:1, 9:1, 1:0) to obtain 16 fractions (Fr.1–Fr.16). Fr.4 (0.88 g) was separated by silica gel CC (petroleum ether/EtOAc, 50:1–5:2) to afford 12 subfractions (Fr.4.1–Fr.4.12), Fr.4.5 was purified by silica gel CC (petroleum ether/EtOAc, 50:4) to yield compound **6** (3.5 mg). Purification of subfraction Fr.4.6 using silica gel CC (petroleum ether/EtOAc, 50:4) furnished compound **10** (3.3 mg). Fr.5 (5.3 g) was applied to silica gel CC eluted by petroleum ether/EtOAc (1:0–5:1), yielding 15 subfractions (Fr.5.1–Fr.5.15). Separation of Fr.5.2 by silica gel CC (petroleum ether/CHCl₃/EtOAc, 50:10:1) afforded compounds **1** (2.9 mg) and **5** (3.2 mg). Compounds **2** (2.9 mg) and **3** (2.8 mg) were obtained by separation of subfraction Fr.5.3 with silica gel CC (petroleum ether/EtOAc/isopropyl alcohol, 100:10:1). Subfraction Fr.5.4 was separated by silica gel CC (petroleum ether/CHCl₃/isopropyl alcohol, 100:10:1) and preparative TLC, yielding compounds **9** (2.2 mg) and **4** (1.2 mg). Subfraction Fr.5.7 was chromatographed by silica gel CC (petroleum ether/CHCl₃/isopropyl alcohol, 100:15:1) to obtain compounds **7** (1.2 mg) and **8** (2.3 mg). Fr.6 (0.6 g) was fractionated by silica gel CC (petroleum ether/CHCl₃/CH₃OH, 2:1:1), leading to isolation of 7 subfractions (Fr.6.1–Fr.6.7). Isolation of subfraction Fr.6.6 using silica gel CC and semi-preparative HPLC obtained compounds **15** (18.0 mg) and **16** (5.4 mg). Fr.7 (1.3 g) was divided into 13 subfractions (Fr.7.1–Fr.7.13) by silica gel CC using petroleum ether/EtOAc (500:1–0:1) as eluent. Subfraction Fr.7.11 was isolated via silica gel CC and semi-preparative HPLC to yield compounds **12** (2.2 mg) and **13** (3.0 mg). Fr.8 (0.8 g) was purified by silica gel CC (petroleum ether/EtOAc, 200:1–0:1), affording compounds **11** (0.8 mg) and **14** (3.5 mg).

Table 1. ^1H NMR (500 MHz) data for compounds 1–6.

| position | 1 ^a | 2 ^a | 3 ^a | 4 ^b | 5 ^a | 6 ^a |
|----------|----------------------|----------------------|----------------|----------------------|----------------------|----------------------|
| 2 | 2.20, m | 1.76, m | 2.12, m | 1.73, m | 1.77, m | 1.94, m |
| 3a | 1.84, m | 1.85, m | 1.88, m | 1.76, m | 1.80, m | 2.38, dd (12.5, 7.1) |
| 3b | 1.22, m | 1.14, m | 1.14, m | 1.04, m | 1.25, m | 1.36, m |
| 4a | 1.70, m | 1.53, m | 1.59, m | 1.42, m | 2.24, dd (17.2, 9.1) | 4.29, t (7.3) |
| 4b | | | 1.50, m | | 2.11, m | |
| 5 | 1.66, m | 1.54, m | 1.74, m | 1.64, dd (11.7, 8.5) | | |
| 7 | | 1.80, m | | | | |
| 8 | 2.72, d (7.0) | | 1.87, m | 2.18, dd (6.6, 4.7) | 2.13, dd (7.5, 5.6) | 1.83, m |
| 9a | 2.18, m | 2.00, m | 1.92, m | 1.53, m | 1.81, m | 1.83, m |
| 9b | 1.65, m | 1.56, m | 1.60, m | | 1.63, m | 1.66, m |
| 10a | 1.74, m | 1.55, m | 1.68, m | 1.15, m | 1.42, m | 1.67, m |
| 10b | 1.53, m | 1.26, m | 1.32, m | | 1.18, m | 1.51, m |
| 11a | 3.34, m | 1.89, d (10.1) | 4.01, brs | 1.54, d (10.4) | 1.57, dd (10.5, 5.5) | 1.49, t (7.7) |
| 11b | | 1.09, dt (10.1, 2.2) | | 1.25, dd (10.4, 4.8) | 1.32, m | 1.30, m |
| 12a | 3.53, t (10.7) | 0.87, d (6.7) | 1.01, d (6.9) | 0.81, d (6.1) | 0.95, d (6.5) | 3.70, dd (10.6, 6.1) |
| 12b | 3.42, dd (10.7, 4.5) | | | | | 3.55 dd (10.6, 7.7) |
| 13a | 4.81, d (1.5) | 3.89, dd (11.1, 9.4) | 1.19, s | 3.40, d (4.5) | 3.60, d (10.9) | 1.06, s |
| 13b | 4.79, d (1.5) | 3.77, dd (11.1, 2.7) | | | 3.54 d (10.9) | |
| 14 | 1.13, s | 1.06, s | 0.87, s | 0.85, s | 1.07, s | 1.03, s |
| 15 | 1.10, s | 0.79, s | 0.95, s | 0.80, s | 1.41, s | 1.60, s |

^aRecorded in CD_3OD , ^bRecorded in DMSO-d_6 .

Agarozizanol A (1)

Colorless crystals; $[\alpha]_{25\text{D}} -3$ (c 0.28, MeOH); IR (KBr) ν_{max} cm^{-1} : 3252, 2956, 2870, 1629, 1462, 1090, and 1044; ^1H and ^{13}C NMR data, see Tables 1 and 2; HRESIMS m/z 259.1667 $[\text{M} + \text{Na}]^+$ (calcd for $\text{C}_{15}\text{H}_{24}\text{NaO}_2$, 259.1669); 1D and 2D NMR, IR spectra, and HRESIMS, see Figure S2–S9 in Supplementary material.

Agarozizanol B (2)

Colorless crystals; $[\alpha]_{25\text{D}} +15$ (c 0.28, MeOH); IR (KBr) ν_{max} cm^{-1} : 3413, 2956, 2870, 1450, 1381, 1261, and 1059; ^1H and ^{13}C NMR data, see Tables 1 and 2; HRESIMS m/z 261.1820 $[\text{M} + \text{Na}]^+$ (calcd for $\text{C}_{15}\text{H}_{26}\text{NaO}_2$, 261.1825). 1D and 2D NMR, IR spectra, and HRESIMS, see Figures S10–S17 in Supplementary material.

Agarozizanol C (3)

White amorphous powder; $[\alpha]_{25\text{D}} -11$ (c 0.25, MeOH); IR (KBr) ν_{max} cm^{-1} : 3444, 2956, 2868, 1456, 1376, 1250, 1091, and 1027; ^1H and ^{13}C NMR data, see Tables 1 and 2; HRESIMS m/z 261.1817 $[\text{M} + \text{Na}]^+$ (calcd for $\text{C}_{15}\text{H}_{26}\text{NaO}_2$, 261.1825). 1D and 2D NMR, IR spectra, and HRESIMS, see Figure S18–Figure S25 in Supplementary material.

Agarozizanol D (4)

White amorphous powder; $[\alpha]_{25\text{D}} +14$ (c 0.10, MeOH); IR (KBr) ν_{max} cm^{-1} : 3439, 2950, 2867, 1457, 1374, and 1067; ^1H and ^{13}C NMR data, see Table 1 and 2; HRESIMS m/z 261.1826 $[\text{M} + \text{Na}]^+$ (calcd for $\text{C}_{15}\text{H}_{26}\text{NaO}_2$, 261.1825). 1D and 2D NMR, IR spectra, and HRESIMS, see Figure S26–S33 in Supplementary material.

Agarozizanol E (5)

White amorphous powder; $[\alpha]_{25\text{D}} -7$ (c 0.33, MeOH); IR (KBr) ν_{max} cm^{-1} : 3447, 2938, 2863, 1627, 1456, 1377, 1260, 1094, and 1034; ^1H and ^{13}C NMR data, see Tables 1 and 2; HRESIMS m/z 243.1707 $[\text{M} + \text{Na}]^+$ (calcd for $\text{C}_{15}\text{H}_{24}\text{NaO}$, 243.1719). 1D and 2D NMR, IR spectra, and HRESIMS, see Figure S34–S41 in Supplementary material.

Table 2. ^{13}C NMR (125 MHz) data for compounds 1–6.

| position | 1 ^a | 2 ^a | 3a | 4 ^b | 5 ^a | 6 ^a |
|----------|----------------------|---------------------|---------------------|---------------------|---------------------|---------------------|
| 1 | 58.4, C | 53.0, C | 57.0, C | 51.9, C | 54.0, C | 52.3, C |
| 2 | 47.5, CH | 40.2, CH | 39.3, CH | 38.7, CH | 41.1, CH | 44.7, CH |
| 3 | 25.8, CH_2 | 31.5, CH_2 | 33.0, CH_2 | 30.5, CH_2 | 33.5, CH_2 | 35.9, CH_2 |
| 4 | 22.3, CH_2 | 21.9, CH_2 | 23.3, CH_2 | 20.7, CH_2 | 28.4, CH_2 | 81.3, CH |
| 5 | 59.1, CH | 60.4, CH | 56.7, CH | 55.6, CH | 146.7, C | 143.1, C |
| 6 | 37.4, C | 35.8, C | 40.2, C | 37.4, C | 126.1, C | 137.0, C |
| 7 | 162.6, C | 58.1, CH | 80.3, C | 76.1, C | 46.5, C | 41.9, C |
| 8 | 55.4, CH | 83.6, C | 58.4, CH | 43.0, CH | 43.0, CH | 48.0, CH |
| 9 | 27.9, CH_2 | 21.8, CH_2 | 24.4, CH_2 | 25.5, CH_2 | 25.1, CH_2 | 25.3, CH_2 |
| 10 | 20.2, CH_2 | 32.2, CH_2 | 20.4, CH_2 | 21.0, CH_2 | 29.7, CH_2 | 39.5, CH_2 |
| 11 | 84.3, CH | 52.2, CH_2 | 83.5, CH | 37.4, CH | 37.8, CH_2 | 30.9, CH_2 |
| 12 | 62.6, CH_2 | 14.4, CH_3 | 18.4, CH_3 | 19.1, CH_3 | 14.4, CH_3 | 64.3, CH_2 |
| 13 | 108.2, CH_2 | 62.4, CH_2 | 23.9, CH_3 | 62.7, CH_2 | 66.7, CH_2 | 28.6, CH_3 |
| 14 | 27.9, CH_3 | 33.9, CH_3 | 27.6, CH_3 | 27.8, CH_3 | 23.3, CH_3 | 25.4, CH_3 |
| 15 | 32.1, CH_3 | 17.8, CH_3 | 21.8, CH_3 | 14.5, CH_3 | 13.3, CH_3 | 12.8, CH_3 |

^aRecorded in CD_3OD , ^bRecorded in DMSO-d_6 .

Agarozizanol F (6)

White amorphous powder; $[\alpha]_{25\text{D}} +2$ (c 0.36, MeOH); IR (KBr) ν_{max} cm^{-1} : 3446, 2928, 2867, 1617, 1454, 1382, and 1084; ^1H and ^{13}C NMR data, see Tables 1 and 2; HRESIMS m/z 259.1662 $[\text{M} + \text{Na}]^+$ (calcd for $\text{C}_{15}\text{H}_{24}\text{NaO}_2$, 259.1669). 1D and 2D NMR, IR spectra, and HRESIMS, see Figure S42–S49 in Supplementary material.

X-ray crystallographic analysis of compound 2

A suitable crystal of **2** obtained from MeOH was selected and determined on a Bruker D8 QUEST diffractometer at 296.15 K. Crystal data for compound **2**: $\text{C}_{15}\text{H}_{26}\text{O}_2$ ($M = 238.36$ g/mol), orthorhombic, space group $P2_12_12_1$, $a = 6.7545(7)$ Å, $b = 8.8069(8)$ Å, $c = 23.886(2)$ Å, $V = 1420.9$ (2) Å³, $Z = 4$, $T = 296(2)$ K, μ (Cu $K\alpha$) = 0.556 mm^{-1} , $D_{\text{calc}} = 1.114$ g/cm^3 , 9320 reflections collected ($7.402^\circ \leq 2\theta \leq 136.888^\circ$), 2598 unique ($R_{\text{int}} = 0.1110$, $R_{\text{sigma}} = 0.0937$). The final $R1$ was 0.0559 ($I > 2\sigma(I)$) and $wR2$ was 0.1624 (all data), Flack parameter = 0.3(8). The crystallographic data for **2** have been deposited at the Cambridge Crystallographic Data Centre under the reference number CCDC 1873716. This data can be obtained free of charge via <http://www.ccdc.cam.ac.uk/conts/retrieving.html> or from CCDC, 12 Union Road, Cambridge, CB21EZ, UK; (fax: +44-(0)1223-336033 or e-mail: deposit@ccdc.cam.ac.uk).

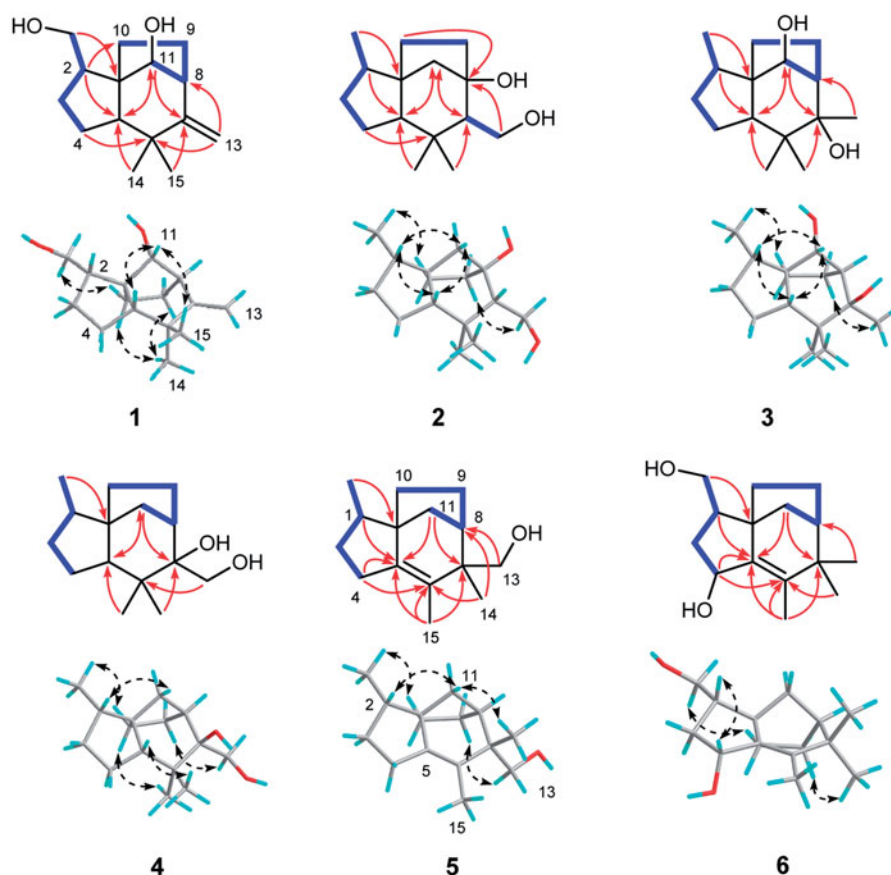


Figure 2. Key ^1H - ^1H COSY (bold lines), HMBC (arrows), and ROESY (dashed double arrows) correlations of compounds 1–6.

α -Glucosidase inhibitory assay

The α -glucosidase (G5003, Sigma-Aldrich) was obtained from *Saccharomyces cerevisiae* and the enzyme inhibitory assay was performed using formerly described method²⁴ with some modifications. The samples were dissolved in DMSO and 2-fold diluted to afford a serial concentrations (the highest final concentration was set at 750 μM because of low solubility of 1–10 in buffer). 10 μL sample was incubated with 100 μL α -glucosidase solution (0.2 U/mL in 100 mM phosphate buffer (pH: 6.8)) at 37 $^\circ\text{C}$ for 15 min. Then, 40 μL of 2.5 mM *p*-nitrophenyl- α -D-glucopyranoside (*p*-NPG) were added and further incubated at 37 $^\circ\text{C}$ for 15 min. DMSO instead of compound was used as control and the blank wells contained buffer in place of substrate. The OD values were measured at 405 nm with microplate reader. Acarbose was used as reference compound. The percentage inhibition was calculated using the following equation:

$$\% \text{ inhibition} = [1 - (\text{OD}_{\text{compound}} - \text{OD}_{\text{blank}}) / (\text{OD}_{\text{control}} - \text{OD}_{\text{blank}})] \times 100$$

Tyrosinase inhibitory assay

All the isolated compounds (1–16) were tested for the inhibitory activity against tyrosinase (T3824, Sigma-Aldrich) from mushroom according to the previously reported method¹⁶ with slight modifications. Briefly, 130 μL of tyrosinase (50 U/mL) solvated in 50 mM phosphate buffer (pH: 6.8) were mixed with 20 μL of 2-fold serial dilutions (from 1 mM to 0.03125 mM) of compounds in DMSO, and transferred into a 96-well plate. After 5 min pre-incubation of the mixture at 37 $^\circ\text{C}$, 50 μL of 2 mM L-tyrosine in buffer were added

and incubated for additional 20 min at 37 $^\circ\text{C}$. The control wells contained DMSO instead of compound, and the blank wells were added with buffer in place of L-tyrosine. Kojic acid was used as a positive control. The absorbance was measured at 495 nm using microplate reader. The percentage inhibition was calculated using the formula as below:

$$\% \text{ inhibition} = [1 - (\text{OD}_{\text{compound}} - \text{OD}_{\text{blank}}) / (\text{OD}_{\text{control}} - \text{OD}_{\text{blank}})] \times 100$$

Kinetic analysis

To determine the mechanisms by which the most effective compound 5 inhibited α -glucosidase and compound 14 inhibited tyrosinase, the enzyme kinetic analysis was investigated at various concentrations of substrate (2.5, 1.25, 0.625, and 0.3125 mM *p*-NPG for α -glucosidase; 4.0, 2.0, 1.0, and 0.5 mM tyrosine for tyrosinase) in the absence or presence of different test inhibitor concentrations (0, 187.5, and 750 μM of 5; 0, 25, and 100 μM of 14) according to the inhibition assay described above. The data were expressed as double-reciprocal Lineweaver–Burk plot and the inhibition constants (K_i and K_{iS}) were obtained from secondary plots of slope and y intercept of lines from Lineweaver–Burk plot against inhibitor²⁵.

Molecular docking study

The X-ray structures of mushroom tyrosinase (PDB: 2Y9X) at a resolution of 2.78 \AA and α -glucosidase (PDB: 3A4A) co-crystallized with glucose at a resolution of 1.6 \AA were achieved from RCSB Protein Data Bank (www.rcsb.org). All hydrogen atoms and

gasteiger charges in the protein structure were added by AutoDockTools and molecular docking simulations were performed with Autodock 4.2 software using the Lamarckian Genetic Algorithm^{26,27}. Compounds **5** and **10** were docked into the catalytic site of α -glucosidase with a grid box of 50 Å × 50 Å × 50 Å at 0.375 Å space, centered at coordinates of $x=21.275$, $y=-0.741$, and $z=18.635$. Genetic Algorithm parameters were set at Runs 50 and the maximum number of evals was set as medium (25000000). For the compounds **13** and **14**, mixed type tyrosinase inhibitors, a blind molecular docking simulation was performed (Runs 20 and the maximum number of evals was set as short (250000)). The size of grid box was set at 100 Å × 100 Å × 100 Å in the x , y , and z dimensions at 0.375 Å space. This computational docking identified the site that bound tightly to the ligand. Then, a refined docking simulation was conducted with smaller grid box of 30 Å × 44 Å × 30 Å at 0.375 Å space, centered at the above identified binding site ($x=-16.345$, $y=-36.541$, $z=-22.916$). The Genetic Algorithm parameters were set at Runs 50 and the maximum number of evals was set as medium (25000000). The predicted geometries were ranked by the binding energies and clustered at RMSD value of 2 Å, and the best pose was selected for further analysis.

Results and discussion

Structure elucidation

Compound **1** was obtained as colorless crystals and its molecular formula was assigned to be $C_{15}H_{24}O_2$ based on the HRESIMS ion peak $[M+Na]^+$ at m/z 259.1667 (calcd for $C_{15}H_{24}NaO_2$, 259.1669), requiring 4 degrees of unsaturation. The 1H NMR data (Table 1) of **1** showed resonances for two methyl groups at δ_H 1.10 (3H, s) and 1.13 (3H, s), two exocyclic olefinic protons at δ_H 4.81 (1H, d, $J=1.5$ Hz) and 4.79 (1H, d, $J=1.5$ Hz), and one oxygenated methylene at δ_H 3.53 (1H, t, $J=10.7$ Hz) and 3.42 (1H, dd, $J=10.7$, 4.5 Hz). The ^{13}C NMR data (Table 2) of **1** showed fifteen carbon signals which were categorized by HSQC spectrum as two methyl groups, six methylenes (one oxygenated), four methines, and three quaternary carbons. Apart from the double bond (δ_C 162.6, 108.2), the remaining three degrees of unsaturation combined with above mentioned spectroscopic data implied that **1** was a tricyclic sesquiterpenoid. In the 1H - 1H COSY spectrum (Figure 2), two spin systems were observed: H_2 -12- H_2 -3- H_2 -4 and H -11- H -8- H_2 -9- H_2 -10. The two spin systems in association with key HMBC correlations from H_2 -12 to C-1, from H_2 -4 to C-1, C-5, and C-6, from H-5 to C-6, C-7, C-1, C-10, and C-11, from H_2 -13 to C-6, C-7, and C-8, and from H_3 -14 and H_3 -15 to C-5, C-6, and C-7 constructed the planar structure of **1**, possessing a prezizaane skeleton, as shown in Figure 1.

The relative configuration of **1** was clarified unambiguously from analysis of the ROESY spectrum. The ROE cross peak of H_2 -12 with H-10a revealed that H_2 -12 and H-10a located at the same side and assumed that they were α oriented. H-11 showed ROESY correlations with H-5 and H_3 -14, indicating they were cofacial and assigned to be β orientation. Thus, the structure of **1** was determined to be as shown in Figure 1, named Agarozizanol A.

Compound **2** was isolated as colorless crystals and had a molecular formula $C_{15}H_{26}O_2$ on the basis of its HRESIMS and ^{13}C NMR spectroscopic data. The 1H NMR data (Table 1) of **2** revealed the presence of three methyl group at δ_H 0.87 (3H, d, $J=6.7$ Hz), 1.06 (3H, s), and 0.79 (3H, s) and one oxygenated methylene at δ_H 3.89 (1H, dd, $J=11.1$, 9.4 Hz) and 3.77 (1H, d, $J=11.1$, 2.7 Hz). The ^{13}C NMR (Table 2) and HSQC spectra of **1** showed the resonances

for three methyl groups, six methylenes (one oxygenated), three methines, and three quaternary carbons (one oxygenated). The aforementioned spectroscopic data were similar to those of **8**, a co-occurring known prezizaane sesquiterpenoids Jinkohol II²⁸. The only difference was the presence of additional oxidized quaternary carbon signal (δ_C 83.6) and the absence of a methine signal in the NMR spectra of **2**. The HMBC correlations (Figure 2) of H_2 -13, H_2 -11, and H_2 -10 with this carbon suggested that the oxygenated carbon was C-8. H_3 -12 showed ROESY correlations with H-10a, suggesting they were cofacial. Other ROESY interactions of H-2 with H-5, H-11b and H_3 -14 with H-5 and H-7 were found, revealing that these protons were resided on the same face. Therefore, the structure of **2** was deduced as Agarozizanol B shown in Figure 1.

Compound **3**, a white amorphous powder, was found to have a molecular formula of $C_{15}H_{26}O_2$ from the ion peak $[M+Na]^+$ at m/z 261.1817 (calcd for $C_{15}H_{26}NaO_2$, 261.1825) in the HRESIMS. The 1H and ^{13}C NMR data (Table 1 and 2) of **3** exhibited the characteristic signals for prezizaane sesquiterpenoid including four methyls, four methylenes, four methines, and three quaternary carbons. The NMR spectroscopic data of **3** closely resemble that of **7**, Jinkohol I²⁹, with exception of deshielded C-11 at δ_C 83.5. This chemical shift indicated the attachment of a hydroxyl to C-11, which was confirmed by HMBC correlation from H-11 to C-9/C-10/C-5/C-7 and 1H - 1H COSY correlations of H-11-H-8-H-9- H_2 -10 (Figure 2). The ROESY correlations of H-2/H-11/H-5 suggested that these protons were cofacial and β oriented. Additional ROESY cross peaks of H_3 -12/H-10a and H_3 -13/H-9b permitted assignment of α orientation to H_3 -12 and H_3 -13. Summarizing these data, the structure of **3** was determined as shown in Figure 1 and named Agarozizanol C.

Obtained as white amorphous powder, compound **4** showed an ion peak $[M+Na]^+$ at m/z 261.1826 (calcd for $C_{15}H_{26}NaO_2$, 261.1825) in the HRESIMS, consistent with a molecular formula of $C_{15}H_{26}O_2$. The structure of **4** was similar to that of known compound **7**, except for the presence of additional hydroxyl at C-13 in **4**, which was verified by the deshielded chemical shift of C-13 at δ_C 62.7 and the molecular formula of **4** with one more oxygen atom than that of **7**. The ROESY interactions of H_3 -12 with H_2 -10, H_2 -9 with H_2 -13 and H_3 -15 (Figure 2), indicated these protons located at the same side of the molecule and were assigned to be α oriented. While H-5, H_3 -14, H-2, and H-11_a were oriented on the other side by their ROESY correlations. Hence, the structure of **4** was established as a new epimer of synthetic (+)-prezizaene diol³⁰, named Agarozizanol D.

Compound **5** was obtained as white amorphous powder and was shown to have a molecular formula $C_{15}H_{24}O$ based on its ion peak $[M+Na]^+$ at m/z 243.1707 (calcd for $C_{15}H_{24}NaO$, 243.1719) in HRESIMS. Resonances of three methyls at δ_H 0.95 (3H, d, $J=6.5$ Hz), 1.07 (3H, s), and 1.41 (3H, s), and one oxygenated methylene at δ_H 3.60 (1H, d, $J=10.9$ Hz) and 3.54 (1H, d, $J=10.9$ Hz) were observed in the 1H NMR spectrum of compound **5**. The ^{13}C NMR (Table 2) and HSQC spectra of **5** showed the presence of three methyl groups, six methylenes (one oxygenated), two methines, and four quaternary carbons including two olefinic carbons. These spectroscopic data of **5** were similar to those of compound **10**³¹, a known zizaene sesquiterpenoid. The major difference was that the hydroxyl, which located at C-12 in the **10**, was attached to the C-13 in the compound **5**. This assignment was confirmed by the deshielded chemical shifts of C-13 at δ_C 66.7 and the HMBC correlations between H_2 -13 and C-6/C-14/C-7/C-8 (Figure 2). The ROESY correlations of H_3 -12/H-10a, H_2 -13/H-9a, and H_3 -14/H-11b were observed, allowing the assignment of α

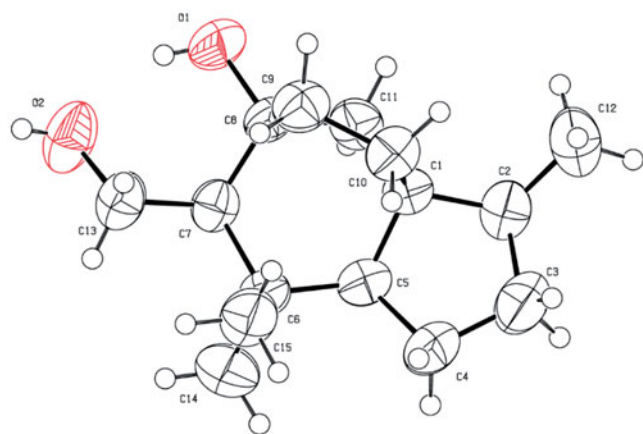


Figure 3. X-ray crystallographic structure of **2**.

orientation for H₃-12 and H-9a, and β orientation for H₃-14 and H-11b. Based on all the above evidence, the structure of **5** was identified as shown in Figure 1 and named as Agarozizanol E.

Compound **6** was obtained as white amorphous powder and displayed an ion peak $[M+Na]^+$ at m/z 259.1662 (calcd for C₁₅H₂₄NaO₂, 259.1669) in its HRESIMS, corresponding to a molecular formula C₁₅H₂₄O₂ with one more oxygen atom than that of **10**. The ¹H and ¹³C NMR data of **6** were closely similar to those of **10**³¹ with only difference being the deshielded chemical shift of CH-4 (δ_H 4.29, δ_C 81.3), which indicated the presence of hydroxyl at C-4. This deduction was further verified by HMBC correlations of H-4 with C-1/C-5/C-6 (Figure 2). The α orientation of CH₂OH-12, OH-4, and CH₂-10 was assigned from the ROESY correlations of H₂-12/H-10b and H-2/H-4. Accordingly, the structure of **6** was characterized as shown in Figure 1, named Agarozizanol F.

On the basis of their structural similarity, compounds **1–6** should be generated from a common precursor in their biosynthetic pathway (Supplementary material, Figure S1), and possessed the same stereochemistry at C-1 and C-2. Fortunately, single-crystals of **2** were obtained and subjected to X-ray diffraction experiment with Cu K α radiation (Figure 3). However, the imperfect Flack parameter [0.3(8)] only allowed confirmation of the above deduced planar structure and relative configuration of **2**. Therefore, further effort was needed to determine the absolute configuration of **1–6**.

By comparing their experimental spectroscopic data with reported data in the literature, the known compounds were identified as Jinkohol I (**7**)²⁹, Jinkohol II (**8**)²⁸, Jinkoholic acid (**9**)³², isokhusenol (**10**)³¹, 6-hydroxy-2-[2-(3-methoxy-4-hydroxyphenyl)ethyl]chromone (**11**)³³, 6-methoxy-7-hydroxy-2-[2-(3-hydroxy-4-methoxyphenyl)ethyl]chromone (**12**)³⁴, 6-hydroxy-7-methoxy-2-[2-(3-hydroxy-4-methoxyphenyl)ethyl]chromone (**13**)¹⁴, 6,8-dihydroxy-2-[2-(4-methoxyphenyl)ethyl]chromone (**14**)¹², 8-chloro-2-(2-phenylethyl)-5,6,7-trihydroxy-5,6,7,8-tetrahydrochromone (**15**)³⁵, 8-chloro-2-(2-(4-methoxyphenyl)ethyl)-5,6,7-trihydroxy-5,6,7,8-tetrahydrochromone (**16**)³⁶.

Bioactivity assays, kinetic analysis, and molecular docking simulations

α -Glucosidase inhibitory activity assay, kinetic analysis, and molecular docking study

All the isolated compounds were assessed for the inhibition against α -glucosidase. The results were listed in the Table 3. Compounds **5**, **7**, **8**, and **10** showed inhibitory effect on

Table 3. α -Glucosidase inhibitory activities of compounds **1–16**^a.

| Compound | α -glucosidase inhibitory activity ^b | |
|-----------------------|--------------------------------------------------------|--------------------------------------|
| | 750 μ M (%) | IC ₅₀ \pm SD (μ M) |
| 1 | 37.4 \pm 1.4 | N.T. |
| 2 | 42.0 \pm 2.7 | N.T. |
| 4 | 49.9 \pm 1.8 | N.T. |
| 5 | 93.4 \pm 3.1 | 112.3 \pm 4.5 |
| 7 | 86.9 \pm 0.4 | 407.0 \pm 3.3 |
| 8 | 77.3 \pm 1.0 | 524.5 \pm 2.7 |
| 9 | 48.9 \pm 1.1 | N.T. |
| 10 | 92.1 \pm 3.4 | 218.8 \pm 5.6 |
| acarbose ^c | 50.7 \pm 1.2 | 743.4 \pm 3.3 |

^aCompounds **3**, **6**, and **11–16** were inactive toward α -glucosidase at 750 μ M (inhibition rate <30%). ^bValues represent means \pm SD based on three individual experiments. ^cPositive control. N.T.: not tested.

α -glucosidase (IC₅₀ values ranging from 112.3 \pm 4.5 to 524.5 \pm 2.7 μ M) superior to acarbose (IC₅₀, 743.4 \pm 3.3 μ M). Compounds **2**, **4**, and **9** also possessed inhibitory activity comparable to the positive control.

To elucidate the type of inhibition of isolated sesquiterpenoids with α -glucosidase, compound **5** with most potency was selected for the kinetic analysis. The Lineweaver-Burk plot (Figure 4(A)) of **5** was established and revealed that K_m and V_{max} decreased in a parallel fashion, indicating that **5** acted as an uncompetitive α -glucosidase inhibitor by binding only with the enzyme-substrate complex³⁷. The inhibition constant was calculated using secondary plot of y intercept versus concentration of inhibitor, yielding K_i value of 168.0 μ M (Figure 4(B)).

In order to rationalize the uncompetitive inhibition mechanism indicated by kinetic study, molecular modeling studies were performed. The most active compounds **5** and **10** were well docked into the catalytic site of the α -glucosidase (Figure 5) with binding energies of -7.2 and -7.1 kcal/mol, respectively. The docking results revealed that compounds **5** and **10** bound to the entrance part of the active site cavity of α -glucosidase, therefore blocking the release of product (glucose) after the enzyme catalyzed reaction was completed³⁷. This may explain why compound **5** behaved as an uncompetitive inhibitor of α -glucosidase. Specifically, compound **5** bound to the active site through hydrogen bonds with residues Asp 352 and Arg 442, and hydrophobic interactions with Tyr 158, Phe 303, and Arg 315 (Figure 5(B)). Compound **10** took hydrogen bonding with Asn 415 and hydrophobic interactions with Lys 156, Phe 314, and Arg 315 (Figure 5(C)). These interactions may provide hints for designing of a new class of α -glucosidase inhibitor.

Tyrosinase inhibitory activity assay, kinetic analysis, and molecular docking study

2-(2-Phenylethyl)chromones **11–16** as well as sesquiterpenoids **1–10** were assayed for the inhibition toward the tyrosinase. As illustrated in Table 4, Compounds **14** and **13** displayed potent inhibitory activity against tyrosinase with IC₅₀ values of 51.5 \pm 0.6 and 89.0 \pm 1.7 μ M, respectively (kojic acid, 46.1 \pm 1.3 μ M). Compound **15** also exhibited weak inhibition effect with inhibition rate of 34.8 \pm 1.4% at 100 μ M. Whereas, compounds **1–12** and **16** were inactive to the tyrosinase up to concentration of 100 μ M (inhibition rate <30%).

As shown in the Lineweaver-Burk plot of the most active compound **14** (Figure 6(A)), increasing inhibitor concentration resulted in a decrease in V_{max} and an increase in K_m , which indicated a

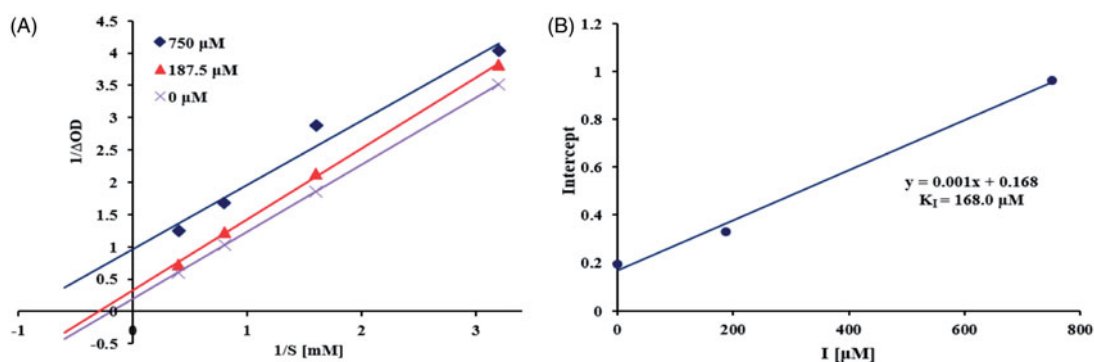


Figure 4. Kinetics of α -glucosidase inhibition by **5**. Lineweaver-Burk plot of **5** against α -glucosidase (A). Secondary plot of y intercept vs. inhibitor for determination of inhibition constant (B).

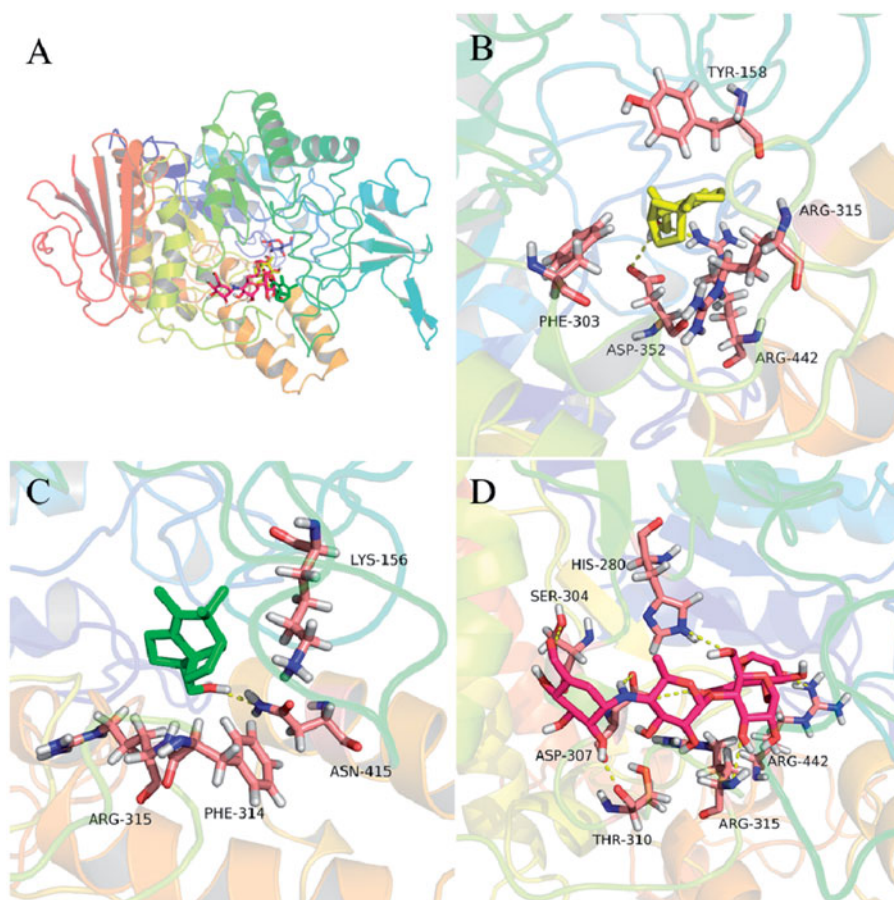


Figure 5. Docking analysis of **5** (yellow sticks), **10** (green sticks), and acarbose (red sticks) with α -glucosidase co-crystallized with glucose (cyan sticks). Binding mode of **5**, **10**, acarbose, and glucose in the active site of α -glucosidase (A). 3D cartoon diagram of the interactions of **5** (B), **10** (C), and acarbose (D) with α -glucosidase.

Table 4. Tyrosinase inhibitory activities of compounds **1–16**^a.

| compound | tyrosinase inhibitory activity ^b | |
|-------------------------|---------------------------------------------|--------------------------------------|
| | 100 μ M (%) | IC ₅₀ \pm SD (μ M) |
| 13 | 53.4 \pm 0.7 | 89.0 \pm 1.7 |
| 14 | 65.0 \pm 1.8 | 51.5 \pm 0.6 |
| 15 | 34.8 \pm 1.4 | N.T. |
| kojic acid ^c | 72.5 \pm 0.5 | 46.1 \pm 1.3 |

^aCompounds **1–12**, and **16** were inactive against tyrosinase at 100 μ M (inhibition rate < 30%). ^bValues represent means \pm SD based on three individual experiments. ^cPositive control. N.T.: not tested.

mixed type inhibition for **14** against tyrosinase²⁵. Thus, compound **14** inhibited the tyrosinase not only by binding with the free enzyme but also with the enzyme–substrate complex.

The inhibition constants of **14** binding with the free enzyme (K_i) and with enzyme-substrate complex (K_{iS}) were determined by the slope and the y intercept versus the inhibitor concentration, respectively. From Figure 6(B,C), the inhibition constants K_i and K_{iS} of **14** were calculated to be 39.6 μ M and 72.8 μ M, respectively, by secondary re-plots, indicating that compound **14** effectively bound to free enzyme as compared to enzyme-substrate complex.

To further gain insight into the binding mechanism of 2-(2-phenylethyl)chromones with tyrosinase, molecular docking simulations were performed. As presented in Figure 7, compounds **13** and **14** were able to anchor the same binding pocket of tyrosinase with the binding energy of -7.49 and -7.75 kcal/mol, respectively. Compound **14** formed hydrogen bonds with residues Gln

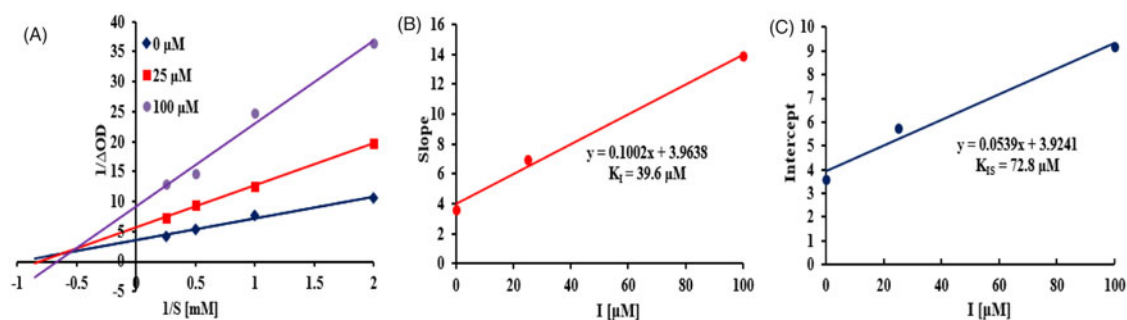


Figure 6. Kinetics of tyrosinase inhibition by **14**. Lineweaver-Burk plot of **14** against tyrosinase (A). Secondary re-plot of slope vs. inhibitor for determination of inhibition constant K_i (B). Secondary re-plot of y intercept vs. inhibitor for determination of inhibition constant K_{is} (C).

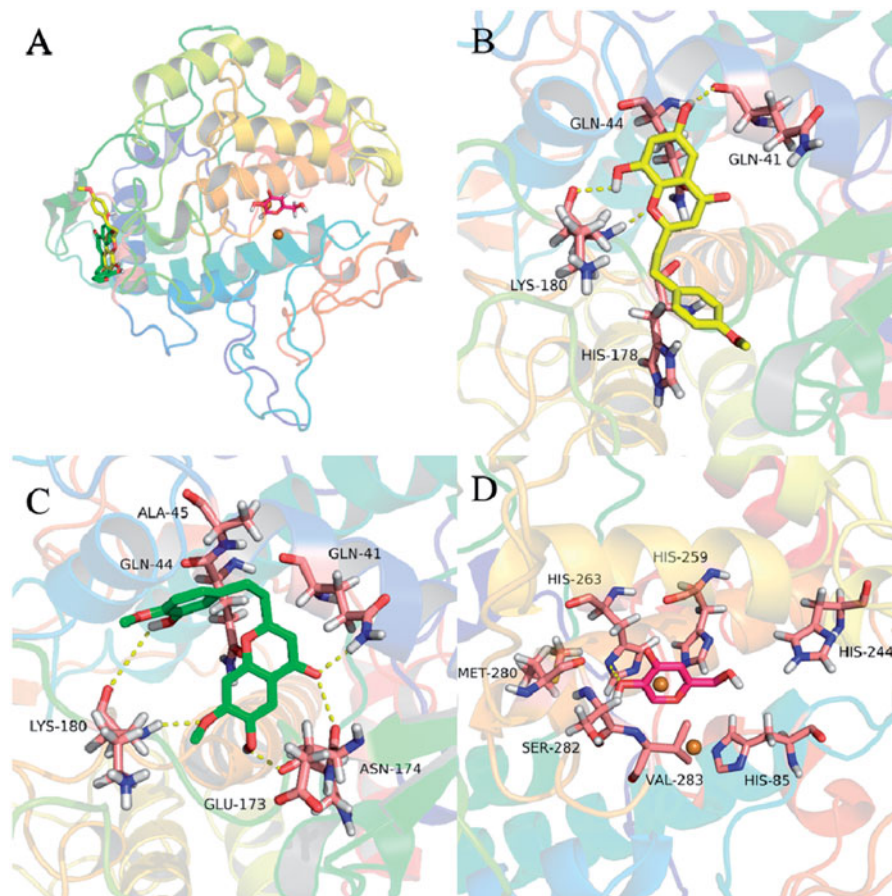


Figure 7. Docking analysis of **13** (green sticks), **14** (yellow sticks), and kojic acid (red sticks) with tyrosinase. Binding mode of **13**, **14**, and kojic acid with tyrosinase (A). 3D cartoon diagram of the interactions of **14** (B), **13** (C), kojic acid (D) with tyrosinase.

41, Lys 180, and hydrophobic interactions with residues His 178 and Gln 44. However, compound **13** bound to the binding site with a different mode and interacted via hydrogen bonds with residues Gln 41, Lys 180, Asn 174, and Glu173, and hydrophobic interactions with residues Gln 44 and Ala 45. The differences may stem from the substitution of ring A and B of 2-(2-phenylethyl)-chromones. These results unveiled a possible allosteric site of tyrosinase by 2-(2-phenylethyl)-chromones and will be helpful for understanding the binding interactions between 2-(2-phenylethyl)-chromones and tyrosinase.

Conclusions

The ethyl ether extract of agarwood from an *Aquilaria* plant afforded 6 previously undescribed sesquiterpenoids, 4 known

sesquiterpenoids, as well as 6 known 2-(2-phenylethyl)chromones. Among them, compounds **2**, **4**, **5**, and **7–10** showed intriguing inhibitory activity against α -glucosidase. The combined enzyme kinetic and molecular docking studies were performed and revealed that the most effective compound **5**, a new zizaane-type sesquiterpenoid, behaved as an uncompetitive α -glucosidase inhibitor and blocked catalytic reaction by interacting with the entrance of active site of α -glucosidase. Uncompetitive inhibitors are considered to be superior to competitive and noncompetitive inhibitors in drug development and are expected to display better *in vivo* efficacy^{37,38}. Therefore, compound **5** could serve as a new promising lead compound for synthesis of more potent derivatives as α -glucosidase inhibitors. Additionally, compounds **13** and **14** manifested remarkable tyrosinase inhibitory effect. Compound **14** with the most potency was revealed to have affinity for the

allosteric site of tyrosinase as a mixed type inhibitor. Agarwood formation is due to a self-defense mechanism initiated by the tree to fight off pests and pathogens invading through holes and wounds on the tree surface⁶. 2-(2-Phenylethyl)chromone is one of the two main components of agarwood and our study revealed the 2-(2-phenylethyl)chromones exert inhibitory activity on tyrosinase, which may provide the chemical evidence for the self-defense mechanism of the agar-producing tree against pests.

Disclosure statement

The authors declare no conflict of interest.

Funding

This work was supported by the Innovative Research Team Grant of the Natural Science Foundation of Hainan Province (No.2017CXTD020), Major Technology Project of Hainan Province (ZDKJ2016004-03), Central Public-interest Scientific Institution Basal Research Fund for Innovative Research Team Program of CATAS (17CXTD-15), and China Agriculture Research System (CARS-21).

References

- Nathan DM. Long-term complications of diabetes mellitus. *N Engl J Med* 1993;328:1676–85.
- Santos-Longhurst A, Krucik G. Type 2 diabetes statistics and facts. Healthline 2014. Available from: www.healthline.com/health/type-2-diabetes/statistics.
- Song YH, Uddin Z, Jin YM, et al. Inhibition of protein tyrosine phosphatase (PTP1B) and α -glucosidase by geranylated flavonoids from *Paulownia tomentosa*. *J Enzyme Inhib Med Chem* 2017;32:1195–202.
- Bojarova P, Kren V. Glycosidases: a key to tailored carbohydrates. *Trends Biotechnol* 2009;27:199–209.
- Israili ZH. Advances in the treatment of type 2 diabetes mellitus. *Am J Ther* 2011;18:117–52.
- Lee SY, Mohamed R. The origin and domestication of *Aquilaria*, an important agarwood-producing genus, Agarwood. Singapore: Springer, 2016;pp.1–20.
- Yang D-L, Wang H, Guo Z-K, et al. A new 2-(2-phenylethyl) chromone derivative in Chinese agarwood 'Qi-Nan' from *Aquilaria sinensis*. *J Asian Nat Prod Res* 2014;16:770–6.
- Hashim YZH-Y, Kerr PG, Abbas P, et al. *Aquilaria* spp. (agarwood) as source of health beneficial compounds: a review of traditional use, phytochemistry and pharmacology. *J Ethnopharmacol* 2016;189:331–60.
- Dai H-F. Research progress of agarwood. Beijing: Science press, 2017.
- Li W, Cai C-H, Guo Z-K, et al. Five new eudesmane-type sesquiterpenoids from Chinese agarwood induced by artificial holing. *Fitoterapia* 2015;100:44–9.
- Huo H-X, Zhu Z-X, Song Y-L, et al. Anti-inflammatory dimeric 2-(2-phenylethyl) chromones from the resinous wood of *Aquilaria sinensis*. *J Nat Prod* 2018;81:543–53.
- Liao G, Mei W-L, Dong W-H, et al. 2-(2-Phenylethyl) chromone derivatives in artificial agarwood from *Aquilaria sinensis*. *Fitoterapia* 2016;110:38–43.
- Yang D-L, Mei W-L, Zeng Y-B, et al. 2-(2-phenylethyl)chromone derivatives in Chinese agarwood "Qi-Nan" from *Aquilaria sinensis*. *Planta Med* 2013;79:141329–34.
- Yang L, Qiao L, Xie D, et al. 2-(2-phenylethyl)chromones from Chinese eaglewood. *Phytochemistry* 2012;76:92–7.
- Yang L, Qiao L, Ji C, et al. Antidepressant abietane diterpenoids from Chinese eaglewood. *J Nat Prod* 2013;76:216–22.
- Kim JH, Cho IS, So YK, et al. Kushenol A and 8-prenylkaempferol, tyrosinase inhibitors, derived from *Sophora flavescens*. *J Enzyme Inhib Med Chem* 2018;33:1048–54.
- Chang TS. An updated review of tyrosinase inhibitors. *Int J Mol Sci* 2009; 10:2440–75.
- Şöhretoğlu D, Sari S, Barut B, et al. Tyrosinase inhibition by some flavonoids: inhibitory activity, mechanism by in vitro and in silico studies. *Bioorg Chem* 2018;81:168–74.
- Olivares C, Solano F. New insights into the active site structure and catalytic mechanism of tyrosinase and its related proteins. *Pigment Cell Melanoma Res* 2009;22:750–60.
- Mcevely JA, Iyengar R, Otwell WS. Inhibition of enzymatic browning in foods and beverages. *Crit Rev Food Sci Nutr* 1992;32:253–73.
- Guerrero A, Rosell G. Biorational approaches for insect control by enzymatic inhibition. *Curr Med Chem* 2005;12:461–9.
- Gorman MJ, An C, Kanost MR. Characterization of tyrosine hydroxylase from *Manduca sexta*. *Insect Biochem Mol Biol* 2007;37:1327–37.
- Xu Y, Stokes AH, Freeman WM, et al. Tyrosinase mRNA is expressed in human substantia nigra. *Mol Brain Res* 1997;1: 4559–162.
- Liu Q-B, Cheng Z-Y, Yan Z-Y, et al. *Prunus tomentosa* seed waste as a source of aromatic glycosides: valuable phytochemicals with α -glucosidase inhibitory and hepatoprotective properties. *Ind Crops Prod* 2018;111:590–6.
- Si Y-X, Ji S, Fang N-Y, et al. Effects of piperonylic acid on tyrosinase: mixed-type inhibition kinetics and computational simulations. *Process Biochem* 2013;48:111706–14.
- Morris GM, Goodsell DS, Halliday RS, et al. Automated docking using a Lamarckian genetic algorithm and an empirical binding free energy function. *J Comput Chem* 1998;19: 1639–62.
- Huey R, Morris GM, Olson AJ, et al. A semiempirical free energy force field with charge-based desolvation. *J Comput Chem* 2007;28:1145–52.
- Nakanishi T, Yamagata E, Yoneda K, et al. Jinkoh-eremol and jinkohol II, two new sesquiterpene alcohols from agarwood. *J Chem Soc Perkin Trans* 1983;1:601–4.
- Nakanishi T, Yamagata E, Yoneda K, et al. Jinkohol, a preziane sesquiterpene alcohol from agarwood. *Phytochemistry* 1981;20:1597–9.
- Sharma MK, Banwell MG, Willis AC. Generation of (+)-prezizanol, (+)-prezizaene, and the *ent*- β -isopipitazol framework via cationic rearrangement of khusiol and related compounds. *Asian J Org Chem* 2014;3:5632–7.
- Komae H, Nigam IC. Essential oils and their constituents. XXXIX. Structures of khusenic acid and isokhusenic acid, two sesquiterpene constituents of oil of vetiver. *J Org Chem* 1968;33:1771–3.
- Raharivelomanana P, Bianchini JP, Faure RA, et al. Jinkoholic acid, a preziane sesquiterpene from *Neocallitropsis pancheri*. *Phytochemistry* 1994;35:1059–60.
- Shao H, Mei W-L, Li W, et al. Chemical constituents of agarwood originating from *Gyrinops salicifolia*. *Nat Prod Res Dev* 2015;27:2046–9.
- Shao H, Mei W-L, Dong W-H, et al. 2-(2-Phenylethyl) chromone derivatives of agarwood originating from *Gyrinops salicifolia*. *Molecules* 2016;21:1313.

35. Yagura T, Ito M, Kiuchi F, et al. Four new 2-(2-phenylethyl)-chromone derivatives from withered wood of *Aquilaria sinensis*. *Chem Pharm Bull* 2003;51:560–4.
36. Huo H-X, Gu Y-F, Sun H, et al. Anti-inflammatory 2-(2-phenylethyl) chromone derivatives from Chinese agarwood. *Fitoterapia* 2017;118:49–55.
37. Song YH, Kim DW, Curtis-Long MJ, et al. Cinnamic acid amides from *Tribulus terrestris* displaying uncompetitive α -glucosidase inhibition. *Eur J Med Chem* 2016;114:201–8.
38. Cornish-Bowden A. Why is uncompetitive inhibition so rare? A possible explanation, with implications for the design of drugs and pesticides. *FEBS Lett* 1986;203:3–6.